

Measurement of a Mean Circumferential Pressure Distribution of a Smooth Cylinder in a Cross Flow in Sub-Critical Reynolds Number Regime

Kay Gemba *

California State University, Long Beach

October 22, 2007

Abstract

It is well known that objects placed in a free stream flow will result in certain flow characteristics. For a circular cylinder the flow characteristics can be characterized by its circumferential pressure distribution which is a function of Reynolds number. This experiment was conducted in the California State University of Long Beach, *CSULB*, windtunnel to determine the drag coefficient of a smooth cylinder due to its circumferential pressure distribution in the sub-critical Reynolds number regime. A smooth cylinder with a diameter of one inch was subjected to two flow speeds ranging from around $13.3 \pm .2 \frac{m}{s}$ to $24.8 \pm .2 \frac{m}{s}$ with corresponding Reynolds numbers between 20,000 and 40,000, respectively. The average coefficient of drag for the cylinder tested was found to be $0.71 \pm .01$. This report presents the findings as well as a discussion of the aerodynamics involved during this testing.

1 Objective

To determine the drag coefficient of a smooth cylinder due to its circumferential pressure distribution in the sub-critical Reynolds number regime. This will be completed through experimentally measuring the pressure at different points on a smooth cylinder inside a windtunnel. Analysis of the data will help determine the drag coefficients.

*aerospace@gemba.org

2 Background and Theory

Flow characteristics around a circular cylinder can be identified with its circumferential pressure distribution which is a function of Reynolds number.

$$Re_d = \frac{\rho U_\infty D}{\mu} = \frac{U_\infty D}{\nu} \quad (1)$$

The Reynolds number is a measure of the ratio of inertia forces to viscous forces. Also, as the Reynolds number increases, flow separates from the cylinder and creates a pressure differential across the cylinder which causes a drag force. An ideal flow would have no flow separation and the viscosity is assumed to be zero, meaning zero drag force. However, in actuality, the viscosity of the fluid causes the flow to separate from the surface of the object creating a maximum pressure at the front, stagnation pressure.

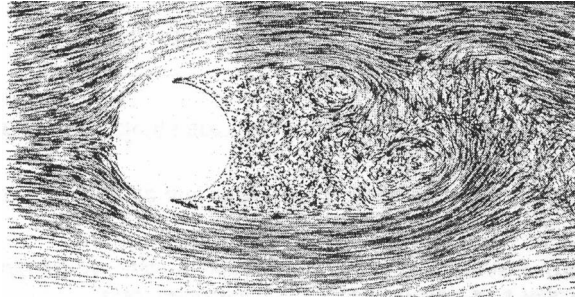


Figure 1: Cylinder in cross flow

The negative pressures at the back of the cylinder results in a net pressure drag on the cylinder. The total drag of the cylinder is the summation of the viscous drag and the pressure drag. In theory, the viscous drag accounts for approximately 5 % of the total drag a smooth cylinder in a cross flow at sub-critical Reynolds number regime. Therefore, viscous drag will be ignored in our calculations. The pressure and drag coefficients are defined as follows:

$$C_P = \frac{P_\theta - P_\infty}{P_0 - P_\infty} = \frac{\Delta P_\theta}{\Delta P_0} \quad (2)$$

$$C_d = \frac{F_D}{\frac{1}{2}\rho U_\infty L} \quad (3)$$

3 Procedure

Experiment two was conducted at CSULB with the Lab Wind Tunnel. The following procedures were used. The wind tunnel was setup by the lab instructor with a circular cylinder of one inch diameter as shown in Figure (2) and Figure (3). A pressure tap on the cylinder was connected to a manometer that was recorded by the computer. The windtunnel was adjusted to an airflow speed. For the given speed, a stagnation pressure was measured. Furthermore, this value determined the free stream velocity. The cylinder was rotated in 10° intervals from 0° to 360° . At each interval the mean pressure differential was recorded ten times using data acquisition software. The procedure was repeated for a different velocity.

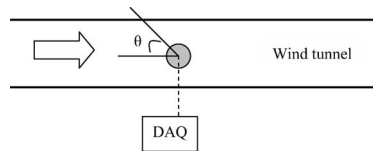


Figure 2: Schematic experimental setup



Figure 3: Windtunnel, CSULB

4 Data

The original data was recorded by a Computer using LABVIEW data acquisition software. Mean values and uncertainties for each point are attached to this report as Attachment No. 1.

5 Calculations

The basic assumption used in all following calculations is that the working fluid, air, is an incompressible fluid. This is a reasonable assumption for low speeds such as those involved in this testing. Standard day atmospheric conditions of air are also used within these calculations. All calculated data is presented within the Tables and Graphs section.

Table 1: Nomenclature, SLS Conditions

C_d	drag coefficient
C_P	pressure coefficient
F_D	drag force
ρ	air density
U_∞	free stream velocity
μ	dynamic viscosity
ν	kinematic viscosity
P_θ	circumferential pressure
P_∞	free stream pressure
P_0	stagnation pressure
ΔP	pressure difference
D	diameter of object

5.1 Free Stream Velocity

The recorded data for the experiment included Pressure readings with the units of in-H²O. This data had to be converted into Pascal's for velocity calculations. Equations (4) and (5) were used for conversion and free stream velocity calculations.

$$\Delta P_{Pascal} = 249 \times \Delta P_{H^2O} \quad (4)$$

$$U_\infty = \sqrt{\frac{\Delta P_{H^2O}}{\frac{1}{2}\rho_{Air,SL}}} = 19.61 \sqrt{\Delta P_{H^2O}} \quad (5)$$

Applying Equation (5), the free stream velocities for the conducted high and low speed experiment are, respectively 24.8 $\frac{m}{s}$ and 13.3 $\frac{m}{s}$.

5.2 Coefficient of Pressure

After calculating the free stream velocity for each data set, the coefficient of pressure C_P is found at each measurement along the circumference of the cylinder, according to equation (2). 36 measurements for ΔP_θ were conducted, starting at $\theta = 0^\circ$ and measuring in 10° increments around the cylinder. Clearly, the ratio of the two pressures is one at the stagnation point. This shows that this is also the point of the maximum pressure differential.

$$C_P = \left(\frac{\Delta P_\theta}{\Delta P_0} \right)_{\theta=0} = 1 \quad (6)$$

5.3 Drag Coefficient

Since the pressure drag is the result of the pressure force in the horizontal direction, the drag coefficient can be obtained from pressure coefficient distribution as:

$$C_d = \frac{1}{2} \int_0^{2\pi} (C_P \cos\theta) d\theta \quad (7)$$

With measurements recorded at 10° increments the coefficient of drag can be approximated linearly by the following equation, using quadrature:

$$C_d = \frac{1}{2} C_P^i \cos(\theta_i) \Delta\theta \quad \text{for } i = 1, 2, \dots, 36$$

All angles are in radians, $\Delta\theta = 0.17453$. For the conducted high and low speed experiment, the coefficients of drag are .76 and .66, respectively.

5.4 Reynolds Number

Having found the free stream velocity earlier it is possible to calculate the Reynolds number for the two flow conditions. Applying equation (1), the calculated Reynolds numbers for the conducted high and low speed experiment are, respectively $4.07E + 04$ and $2.18E + 04$.

5.5 Uncertainty Analysis

In order to get a confidence interval of 95%, we can calculate the error around the mean from our raw data and multiply it by a factor of 2, according to equation (8). For all 36 intervals for each Reynolds number, the maximum of these intervals is chosen to be the confidence interval.

$$CI = 2 \times \sigma = \frac{\sqrt{\sum_{i=1}^n (x_i - \bar{x})^2}}{n - 1} \quad (8)$$

The CI for the higher speed is calculated to be 2.4E-03, for the lower speed is it 4.3E-03. Both intervals are bounded by 5.0E-03, which will be used in following calculations.

Table 2: Calculated Uncertainties

ΔP	$\pm 0.005 \text{ in} - H^2O$
ΔP	$\pm 1.25 \text{ N/m}^2$
D	$\pm 0.005 \text{ in}$
U_∞	$\pm 0.2 \text{ m/s}$
C_P	± 0.007
Re	± 0.7

5.5.1 Sample Calculation

$$U_{\Sigma \cos\theta \Delta\theta} = \sum \cos\left(\frac{\pi}{4 * 180}\right) * 36 = .314$$

$$U_{C_d} = [(U_{\Sigma C_P})^2 + (U_{\Sigma \cos\theta \Delta\theta})^2]^{\frac{1}{2}} = .01$$

6 Graphs and Tables

Calculated Pressure differentials, Pressure coefficients differentials and Drag coefficients are attached to this report as Attachment No. 2 and Attachment No. 3 for High and Low speed, respectively.

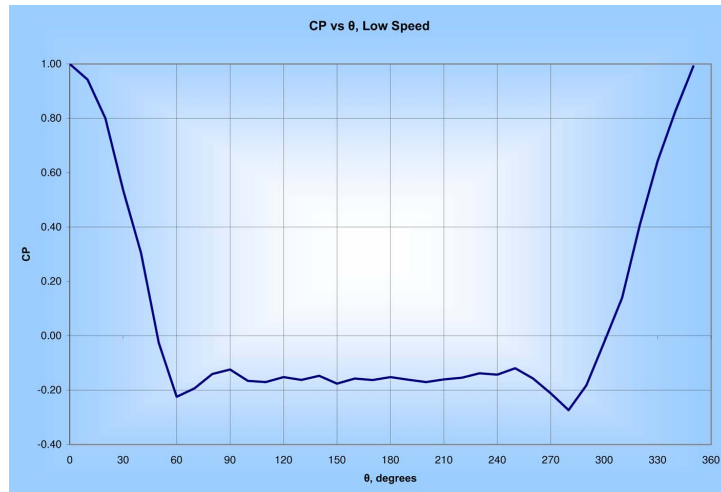


Figure 4: Coefficient of Pressure versus θ , Low speed

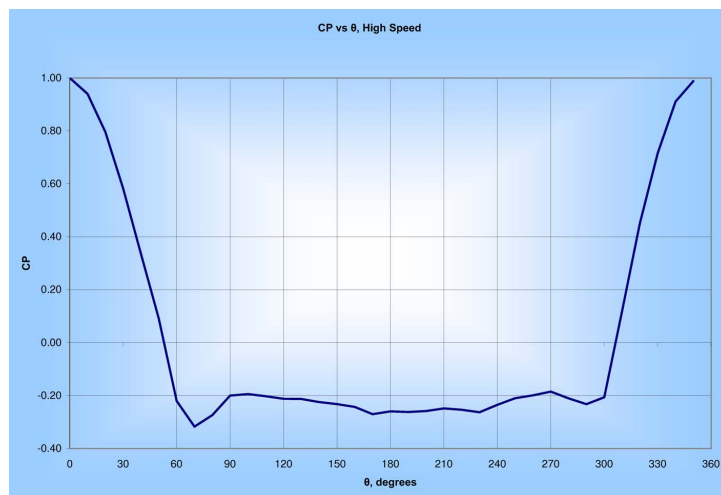
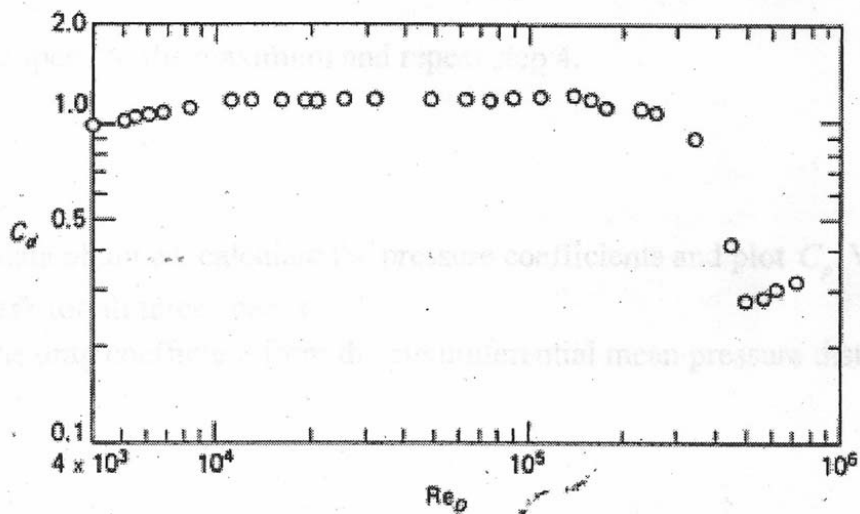


Figure 5: Coefficient of Pressure versus θ , High speed

7 Discussion of results

It can be seen that the velocity at the surface of the cylinder and the local static pressure are both functions of Reynolds Number and θ . Once the pressure distributions have been found the pressure coefficient and the drag coefficient can be found. The pressure coefficient distribution in sub-critical Reynolds number fields remains essentially unchanged in a wide field of Reynolds numbers. The drag coefficients for both speeds are below 1. For the higher Reynolds number it is found to be .76, for the low speed test .66. Comparing these values to theoretical values in Fig. (6), our values are lower than expected. This means that either our measurements are off, neglected viscosity effected are larger than anticipated or we did not have two dimensional flow. Since our expected errors and calculated deviations are relatively small, the difference in the drag coefficient might be assumed to be due to three dimensional flow over the object and therefore a loss of drag on the object. The mean pressure differences plotted versus θ can be seen in



Drag coefficient for a circular cylinder as a function of the Reynolds number. From *Boundary Layer Theory* by Schlichting (1968).

Figure 6:

Fig. (4) and in Fig. (5). The pressure distribution should be theoretically symmetrical with the symmetry axis at $\theta = 180^\circ$. Because the speed and the calculated Reynolds numbers are in the sub-critical stage, the boundary layer around the cylinder was found to be laminar with a certain separation angle. The plot results for the two speed settings show this behavior. These

graphs are very helpful to explain physical effects around the cylinder. For the low speed experiment, we notice an acceleration of the flow until $\theta = 60^\circ$ and a deceleration until 90° . After that, the void area begins because flow is separated. It is slightly varying in the negative Pressure zone, which ends at around 250° . Notice the flow is not completely symmetrical, which might be a source for errors. Comparing these results to the high speed experiment, it can be seen that the separation of flow starts later at $\theta = 70^\circ$ due to a higher momentum of the fluid. It seems that this graph is not symmetrical as well. Since the experiment was only done once for each speed, our data does not support assumptions why this is the case.

The drag coefficients as functions of Reynolds numbers can be compared. As noticed before, the mean values for the drag coefficients were lower than expected, based on comparison with the data from Fig. (6). To approximate the flow as 2-dimensional, the cylinder should have a L/D ratio greater than 150. The L/D for this experiment was far below this value.

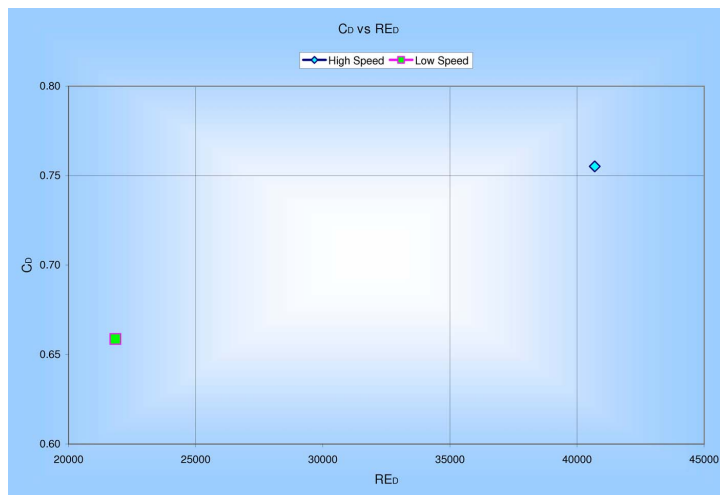


Figure 7: Coefficient of Drag versus Reynolds number

8 Conclusions and recommendations

When the Reynolds number is sufficiently large, the skin friction drag of a bluff body is relatively negligible compared to its form drag. Then the measurement of the drag forces due to normal pressures acting the body will be a good approximation to the total drag. It would have been of advantage to have a wind tunnel setup which is able to generate speeds which can be controlled with ease. It would be useful to take data for double the highest

free stream velocity achieved in this experiment, or at a minimum utilize a greater range of free stream velocities. This would enable more clearly varied separation angles. The mean values for the drag coefficients were lower than expected, based on comparison with published results. Therefore, it would be useful for future study to acquire a setup with a higher L/D ratio. This would enable a closer 2-dimensional flow approximation study. However, the experiment showed different separation points of flow as a function of Reynolds numbers. In addition, the setup proved to be fairly simple to estimate the coefficient of drag.

References

- [1] Dr. Hamid Rahai, MAE 440 Aerodynamics Laboratory Experiments, California State University Long Beach, Spring 2007
- [2] John J. Bertin, Aerodynamics for Engineers, 4th edition, 2002
- [3] Schlichting H. 1979. Boundary-layer theory. 7th ed. New York: McGraw-Hill.